Discovery of biased orientation of human DNA motif sequences affecting enhancer-promoter interactions and transcription of genes

Naoki Osato[1*]

[1]Department of Bioinformatic Engineering, Graduate School of Information Science and Technology, Osaka University, Osaka 565-0871, Japan

[*]Corresponding author

E-mail address: naokiosato11@gmail.com, nosato@ist.osaka-u.ac.jp

Abstract

Chromatin interactions have important roles for enhancer-promoter interactions (EPI) and regulating the transcription of genes. CTCF and cohesin proteins are located at the anchors of chromatin interactions, forming their loop structures. CTCF has insulator function limiting the activity of enhancers into the loops. DNA binding sequences of CTCF indicate their orientation bias at chromatin interaction anchors – forward-reverse (FR) orientation is frequently observed. DNA binding sequences of CTCF were found in open chromatin regions at about 40% - 80% of chromatin interaction anchors in Hi-C and in situ Hi-C experimental data. Though the number of chromatin interactions was about seventy thousand in Hi-C at 50kb resolution, about twenty millions of chromatin interactions were recently identified by HiChIP at 5kb resolution. It has been reported that long range of chromatin interactions tends to include less CTCF at their anchors. It is still unclear what proteins are associated with chromatin interactions.

To find DNA binding motif sequences of transcription factors (TF), such as CTCF, and repeat DNA sequences affecting the interaction between enhancers and promoters of genes and their expression, first I predicted TF bound in enhancers and promoters using DNA motif sequences of TF and experimental data of open chromatin regions in monocytes and other cell types, which were obtained from public and commercial databases. Second, transcriptional target genes of each TF were predicted based on enhancer-promoter association (EPA). EPA was shortened at the genomic locations of FR or reverse-forward (RF) orientation of DNA motif sequence of a TF, which were

supposed to be at chromatin interaction anchors and acted as insulator sites like CTCF. Then, the expression levels of the transcriptional target genes predicted based on the EPA were compared with those predicted from only promoters.

Total 287 biased orientation of DNA motifs (159 FR and 153 RF orientation, the reverse complement sequences of some DNA motifs were also registered in databases, so the total number was smaller than the number of FR and RF) affected the expression level of putative transcriptional target genes significantly in $CD14^+$ monocytes of four people in common. The same analysis was conducted in $CD4^+$ T cells of four people. DNA motif sequences of CTCF, cohesin and other transcription factors involved in chromatin interactions were found to be a biased orientation. Transposon sequences, which are known to be involved in insulators and enhancers, showed a biased orientation. The biased orientation of DNA motif sequences tended to be co-localized in the same open chromatin regions. Moreover, for ~85% of FR and RF orientations of DNA motif sequences, EPI predicted from EPA that were shortened at the genomic locations of the biased orientation of DNA motif sequence were overlapped with chromatin interaction data (Hi-C and HiChIP) significantly more than other types of EPAs.

Keywords: transcriptional target genes, gene expression, transcription factors, enhancer, enhancer-promoter interactions, chromatin interactions, CTCF, cohesin, open chromatin regions, co-location of transcription factors, homodimer, heterodimer, complex

Background

Chromatin interactions have important roles for enhancer-promoter interactions (EPI) and regulating the transcription of genes. CTCF and cohesin proteins are located at the anchors of chromatin interactions, forming their loop structures. CTCF has insulator function limiting the activity of enhancers into the loops (Fig. 1A). DNA binding sequences of CTCF indicate their orientation bias at chromatin interaction anchors – forward-reverse (FR) orientation is frequently observed (de Wit et al. 2015; Guo et al. 2015). About 40% - 80% of chromatin interaction anchors of Hi-C and in situ Hi-C experiments include DNA binding motif sequences of CTCF. Though the number of chromatin interactions was about seventy thousand in Hi-C at 50kb resolution (Javierre et al. 2016), about twenty millions of chromatin interactions were recently identified by HiChIP at 5kb resolution (Mumbach et al. 2017). However, it has been reported that long range of chromatin interactions tends to include less CTCF at their anchors (Jeong et al. 2017). Other DNA binding proteins such as ZNF143, YY1, and SMARCA4 (BRG1) are found to be associated with chromatin interactions and EPI (Bailey et al. 2015; Barutcu et al. 2016; Weintraub et al. 2017). CTCF, cohesin, ZNF143, YY1 and SMARCA4 have other biological functions as well as chromatin interactions and EPI. The DNA binding motif sequences of the transcription factors (TF) are found in open chromatin regions near transcriptional start sites (TSS) as well as chromatin interaction anchors.

DNA binding motif sequence of ZNF143 was enriched at both chromatin interaction anchors. ZNF143's correlation with the CTCF-cohesin cluster relies on its

77 weakest binding sites, found primarily at distal regulatory elements defined by the
78 'CTCF-rich' chromatin state. The strongest ZNF143-binding sites map to promoters
79 bound by RNA polymerase II (POL2) and other promoter-associated factors, such as the
80 TATA-binding protein (TBP) and the TBP-associated protein, together forming a
81 'promoter' cluster (Bailey et al. 2015).

82 DNA binding motif sequence of YY1 does not seem to be enriched at both
83 chromatin interaction anchors (Z-score < 2), whereas DNA binding motif sequence of
84 ZNF143 is significantly enriched (Z-score > 7; Bailey et al. 2015 Figure 2a). In the
85 analysis of YY1, to identify a protein factor that might contribute to EPI, (Ji et al. 2015)
86 performed chromatin immune precipitation with mass spectrometry (ChIP-MS), using
87 antibodies directed toward histones with modifications characteristic of enhancer and
88 promoter chromatin (H3K27ac and H3K4me3, respectively). Of 26 transcription factors
89 that occupy both enhancers and promoters, four are essential based on a CRISPR
90 cell-essentiality screen and two (CTCF, YY1) are expressed in >90% of tissues
91 examined (Weintraub et al. 2017). These analyses started from the analysis of histone
92 modifications of enhancer and promoter marks rather than chromatin interactions. Other
93 protein factors associated with chromatin interactions may be found from other
94 researches.

95 As computational approaches, machine-learning analyses to predict chromatin
96 interactions have been proposed (Schreiber et al. 2017; Zhang et al. 2017). However,
97 they were not intended to find DNA motif sequences of TF affecting chromatin
98 interactions, EPI, and the expression level of transcriptional target genes, which were

99 examined in this study.

100 DNA binding proteins involved in chromatin interactions are supposed to affect
101 the transcription of genes in the loops formed by chromatin interactions. In my previous
102 analysis, the expression level of human putative transcriptional target genes was
103 affected, according to the criteria of enhancer-promoter association (EPA) (Fig. 1B;
104 (Osato 2018)). EPI were predicted based on EPA shortened at the genomic locations of
105 FR orientation of CTCF binding sites, and transcriptional target genes of each TF bound
106 in enhancers and promoters were predicted based on the EPI. The EPA affected the
107 expression levels of putative transcriptional target genes the most among three types of
108 EPAs, compared with the expression levels of transcriptional target genes predicted
109 from only promoters (Fig. 2). The expression levels tended to be increased in
110 monocytes and $CD4^+$ T cells, implying that enhancers activated the transcription of
111 genes, and decreased in ES and iPS cells, implying that enhancers repressed the
112 transcription of genes. These analyses suggested that enhancers affected the
113 transcription of genes significantly, when EPI were predicted properly. Other DNA
114 binding proteins involved in chromatin interactions, as well as CTCF, may locate at
115 chromatin interaction anchors with a pair of biased orientation of DNA binding motif
116 sequences, affecting the expression level of putative transcriptional target genes in the
117 loops formed by the chromatin interactions. As experimental issues of the analyses of
118 chromatin interactions, chromatin interaction data are changed, according to
119 experimental techniques, depth of DNA sequencing, and even replication sets of the
120 same cell type. Chromatin interaction data may not be saturated enough to cover all

121 chromatin interactions. Supposing these characters of DNA binding proteins associated
122 with chromatin interactions and avoiding experimental issues of the analyses of
123 chromatin interactions, here I searched for DNA motif sequences of TF and repeat DNA
124 sequences, affecting EPI and the expression level of putative transcriptional target genes
125 in $CD14^+$ monocytes and $CD4^+$ T cells of four people and other cell types without using
126 chromatin interaction data. Then, putative EPI were compared with chromatin
127 interaction data.
128

129 ## Results

130 **Search for biased orientation of DNA motif sequences**

131 Transcription factor binding sites (TFBS) were predicted using open chromatin
132 regions and DNA motif sequences of transcription factors (TF) collected from various
133 databases and journal papers (see Methods). Transcriptional target genes were predicted
134 using TFBS in promoters and enhancer-promoter association (EPA) shortened at the
135 genomic locations of DNA binding motif sequence of a TF acting as insulator such as
136 CTCF and cohesin (RAD21 and SMC3) (Fig. 1B). To find DNA motif sequences of TF
137 acting as insulator, other than CTCF and cohesin, and repeat DNA sequences affecting
138 the expression level of genes, EPI were predicted based on EPA shortened at the
139 genomic locations of the DNA motif sequence of a TF or a repeat DNA sequence, and
140 transcriptional target genes of each TF bound in enhancers and promoters were
141 predicted based on the EPI. The expression levels of the putative transcriptional target
142 genes were compared with those predicted from promoters using Mann Whiteney U test,

143 two-sided (p-value < 0.05) (Fig. 2A). The number of TF showing a significant
144 difference of expression level of their putative transcriptional target genes was counted.
145 To examine whether the orientation of a DNA motif sequence, which is supposed to act
146 as insulator sites and shorten EPA, affected the number of TF showing a significant
147 difference of expression level of their putative transcriptional target genes, the number
148 of the TF was compared among forward-reverse (FR), reverse-forward (RF), and any
149 orientation (i.e. without considering orientation) of a DNA motif sequence shortening
150 EPA, using chi-square test (p-value < 0.05). To avoid missing DNA motif sequences
151 showing a relatively weak statistical significance by multiple testing collection, the
152 above analyses were conducted using monocytes of four people independently, and
153 DNA motif sequences found in monocytes of four people in common were selected.
154 Total 287 of biased (159 FR and 153 RF) orientation of DNA binding motif sequences
155 of TF were found in monocytes of four people in common, whereas only one any
156 orientation of DNA binding motif sequence was found in monocytes of four people in
157 common (Fig. 2B; Table 1; Supplemental Table S1). FR orientation of DNA motif
158 sequences included CTCF, cohesin (RAD21 and SMC3), ZNF143 and YY1, which are
159 associated with chromatin interactions and EPI. SMARCA4 (BRG1) is associated with
160 topologically associated domain (TAD), which is higher-order chromatin organization.
161 The DNA binding motif sequence of SMARCA4 was not registered in the databases
162 used in this study. FR orientation of DNA motif sequences included SMARCC2, a
163 member of the same SWI/SNF family of proteins as SMARCA4.

164 The same analysis was conducted using DNase-seq data of $CD4^+$ T cells of four

165 people. Total 265 of biased (158 FR and 139 RF) orientation of DNA binding motif
166 sequences of TF were found in T cells of four people in common, whereas only four any
167 orientation (i.e. without considering orientation) of DNA binding motif sequences were
168 found in T cells of four people in common (Supplemental Fig. S1 and Supplemental
169 Table S2). Biased orientation of DNA motif sequences in T cells included CTCF,
170 cohesin (RAD21 and SMC3), ZNF143, YY1, and SMARC. Biased orientation of DNA
171 motif sequences in T cells and monocytes (using H3K27ac histone modification marks,
172 which is described in the next paragraph) included JUNDM2 (JDP2), which is involved
173 in histone-chaperone activity, promoting nucleosome, and inhibition of histone
174 acetylation (Jin et al. 2006). JDP2 forms a homodimer or heterodimer with various TF
175 (https://en.wikipedia.org/wiki/Jun_dimerization_protein). Among 287, 61 of biased
176 orientation of DNA binding motif sequences of TF were found in both monocytes and T
177 cells in common (Supplemental Table S5). For each orientation, 31 FR and 34 RF
178 orientation of DNA binding motif sequences of TF were found in both monocytes and T
179 cells in common. Without considering the difference of orientation of DNA binding
180 motif sequences, 84 of biased orientation of DNA binding motif sequences of TF were
181 found in both monocytes and T cells. As a reason for the increase of the number (84)
182 from 61, a TF or an isoform of the same TF may bind to a different DNA binding motif
183 sequence according to cell types and/or in the same cell type. About 50% or more of
184 alternative splicing isoforms are differently expressed among tissues, indicating that
185 most alternative splicing is subject to tissue-specific regulation (Wang et al. 2008)
186 (Chen and Manley 2009) (Das et al. 2007). The same TF has several DNA binding

187 motif sequences and in some cases one of the motif sequences is almost the same as the
188 reverse complement sequence of another motif sequence of the same TF. For example,
189 RAD21 had both FR and RF orientation of DNA motif sequences, but the number of the
190 FR orientation of DNA motif sequence was relatively small in the genome, and the RF
191 orientation of DNA motif sequence was frequently observed and co-localized with
192 CTCF. I previously found that a complex of TF would bind to a slightly different DNA
193 binding motif sequence from the combination of DNA binding motif sequences of TF
194 composing the complex in *C. elegans* (Tabuchi et al. 2011). From another viewpoint of
195 this study, the expression level of putative transcription target genes of some TF would
196 be different, depending on the genomic locations (enhancers or promoters) of DNA
197 binding motif sequences of the TF in monocytes and T cells of four people.

198 Moreover, using open chromatin regions overlapped with H3K27ac histone
199 modification marks known as enhancer and promoter marks, the same analyses were
200 performed in monocytes and T cells. H3K27ac histone modification marks were used in
201 the analysis of EPI, but were not used in the analysis of TF as insulator like CTCF and
202 cohesin in this study, since new biased orientation of DNA motif sequences were found
203 in this criterion. When H3K27ac histone modification marks were used in the analysis
204 of TF as insulator like CTCF and cohesin, the number of biased orientation of DNA
205 motif sequences was decreased. Total 241 of biased (141 FR and 120 RF) orientation of
206 DNA binding motif sequences of TF were found in monocytes of four people in
207 common, whereas only one any orientation of DNA binding motif sequence was found
208 (Supplemental Table S3). Though the number of biased orientation of DNA motif

209 sequences was reduced, JDP2 was found in monocytes as well as T cells. CTCF,
210 RAD21, SMC3, ZNF143, YY1, and SMARCC2 were also found. For T cells using
211 H3K27ac histone modification marks, total 195 of biased (107 FR and 110 RF)
212 orientation of DNA binding motif sequences of TF were found in T cells of four people
213 in common, whereas only six any orientation of DNA binding motif sequences were
214 found (Supplemental Table S4). Though the number of biased orientation of DNA motif
215 sequences was reduced, CTCF, RAD21, SMC3, YY1, and SMARCC2 were found.
216 Scores of CTCF, RAD21, and SMC3 were increased compared with the result of T cells
217 without using H3K27ac histone modification marks, and they were ranked in the top six.
218 As summary of the results with and without H3K27ac histone modification marks, total
219 386 of biased (223 FR and 214 RF) orientation of DNA motif sequences were found in
220 monocytes of four people in common. Total 348 of biased (202 FR and 198 RF)
221 orientation of DNA motif sequences were found in T cells of four people in common.
222 Total number of these results in monocytes and T cells was 590 biased (368 FR and 359
223 RF) orientation of DNA motif sequences. Biased orientation of DNA motif sequences
224 found in both monocytes and T cells were listed in Supplemental Table S5.

225 To examine whether the biased orientation of DNA binding motif sequences of
226 TF were observed in other cell types, the same analyses were conducted in other cell
227 types. However, for other cell types, experimental data of one sample were available in
228 ENCODE database, so the analyses of DNA motif sequences were performed by
229 comparing with the result in monocytes of four people. Among the biased orientation of
230 DNA binding motif sequences found in monocytes, 69, 82, 56, and 53 DNA binding

231 motif sequences were also observed in H1-hESC, iPS, Huvec and MCF-7 respectively,
232 including CTCF and cohesin (RAD21 and SMC3) (Table 2; Supplemental Table S6).
233 The scores of DNA binding motif sequences were the highest in monocytes, and the
234 other cell types showed lower scores. The results of the analysis of DNA motif
235 sequences in $CD20^+$ B cells and macrophages did not include CTCF and cohesin,
236 because these analyses can be utilized in cells where the expression level of putative
237 transcriptional target genes of each TF show a significant difference between promoters
238 and EPA shortened at the genomic locations of a DNA motif sequence acting as
239 insulator sites. Some experimental data of a cell did not show a significant difference
240 between promoters and the EPA (Osato 2018).

241 Instead of DNA binding motif sequences of TF, repeat DNA sequences were also
242 examined. The expression levels of transcriptional target genes of each TF predicted
243 based on EPA that were shortened at the genomic locations of a repeat DNA sequence
244 were compared with those predicted from promoters. Three RF orientation of repeat
245 DNA sequences showed a significant difference of expression level of putative
246 transcriptional target genes in monocytes of four people in common (Table 3). Among
247 them, LTR16C repeat DNA sequence was observed in iPS and H1-hESC with enough
248 statistical significance considering multiple tests (p-value $< 10^{-7}$). The same as $CD14^+$
249 monocytes, biased orientation of repeat DNA sequences were examined in $CD4^+$ T cells.
250 Three FR and two RF orientation of repeat DNA sequences showed a significant
251 difference of expression level of putative transcriptional target genes in T cells of four
252 people in common (Supplemental Table S7). MIRb and MIR3 were also found in the

253 analysis using open chromatin regions overlapped with H3K27ac histone modification
254 marks, which are enhancer and promoter marks. MIR and other transposon sequences
255 are known to act as insulators and enhancers (Bejerano et al. 2006; Rebollo et al. 2012;
256 de Souza et al. 2013; Jjingo et al. 2014; Wang et al. 2015).
257
258 **Co-location of biased orientation of DNA motif sequences**
259 To examine the association of 287 biased (FR and RF) orientation of DNA
260 binding motif sequences of TF, co-location of the DNA binding motif sequences in open
261 chromatin regions was analyzed in monocytes. The number of open chromatin regions
262 with the same pairs of DNA binding motif sequences was counted, and when the pairs
263 of DNA binding motif sequences were enriched with statistical significance (chi-square
264 test, p-value $< 1.0 \times 10^{-10}$), they were listed (Table 4; Supplemental Table S8; Fig. 3A).
265 Open chromatin regions overlapped with histone modification of enhancer and
266 promoter marks (H3K27ac) (total 26,095 regions) showed a larger number of enriched
267 pairs of DNA motifs than all open chromatin regions (Table 4; Supplemental Table S8;
268 Fig. 3A). H3K27ac is known to be enriched at chromatin interaction anchors (Phanstiel
269 et al. 2017). As already known, CTCF was found with cohesin such as RAD21 and
270 SMC3 (Table 4; Fig. 3A). Top 30 pairs of FR and RF orientations of DNA motifs
271 co-occupied in the same open chromatin regions were shown (Table 4). Total number of
272 pairs of DNA motifs was 492, consisting of 115 unique DNA motifs, when the pair of
273 DNA motifs were observed in more than 80% of the number of open chromatin regions
274 with the DNA motifs. Biased orientation of DNA binding motif sequences of TF tended

275 to be co-localized in the same open chromatin regions.

276 To examine the association of 265 biased orientation of DNA binding motif
277 sequences of TF in $CD4^+$ T cells, co-location of the DNA binding motif sequences in
278 open chromatin regions was analyzed. Top 30 pairs of FR and RF orientations of DNA
279 motifs co-occupied in the same open chromatin regions were shown (Supplemental
280 Table S9; Supplemental Fig. S2). Total number of pairs of DNA motifs was 332,
281 consisting of 118 unique DNA motifs, when the pair of DNA motifs were observed in
282 more than 60% of the number of open chromatin regions with the DNA motifs
283 (chi-square test, p-value $< 1.0 \times 10^{-10}$). Among them, 12 pairs of DNA motif
284 sequences including a pair of CTCF, SMC3, and RAD21 in T cells were found in
285 monocytes in common (Supplemental Table S9).

286

287 **Pairs of biased orientation of DNA motif sequences surrounding genes**

288 CTCF and cohesin are found in chromatin interaction anchors and are considered
289 to form homodimers. TF are also known to form heterodimers with another TF. In this
290 study, if the DNA binding motif sequence of only the mate to a pair of TF was found in
291 EPA, EPA was shortened at one side, which is the genomic location of the DNA binding
292 motif sequence of the mate to the pair, and transcriptional target genes were predicted
293 using the EPA shortened at the side. In this analysis, the mate to both heterodimer and
294 homodimer of TF can be used to examine the effect on the expression level of
295 transcriptional target genes predicted based on the EPA shortened at one side. To
296 examine whether biased orientation of DNA motif sequences tend to be found as a pair

297 of the same TF or different TF in upstream and downstream of genes, the enrichment of
298 pairs of biased orientation of DNA motif sequences was investigated. The number of
299 genes with a pair of FR or RF orientation of DNA motif sequences was counted using
300 all pairs of the DNA motif sequences, and statistical tests (chi-square test) were
301 conducted. The total number of genes (transcripts) with a biased orientation of DNA
302 motif sequence in their upstream or/and downstream was about 20,000. This is almost
303 the same way of analysis as co-location of biased orientation of DNA motif sequences,
304 and the analysis here used the number of genes instead of open chromatin regions. Fig.
305 3B and Supplemental Fig. S3 showed that not only pairs of the same TF, but also pairs
306 of different TF were found in upstream and downstream of genes. DNA motif sequences
307 of CTCF and cohesin (RAD21 and SMC3) were enriched near the same genes, but
308 cohesin tended to be found with another TF near the same genes as well. The number of
309 some pairs of biased orientation of DNA motif sequences in genome sequences was
310 small, though they showed statistical significance (Supplemental material 2). The result
311 of the analysis seems to be different between monocytes and T cells and between using
312 H3K27ac histone modification marks and not using them (Supplemental Fig. S3). Some
313 of these TF would form homodimers or heterodimers directory or indirectly composing
314 a complex structure, contributing to make chromatin interactions (Fig. 5).
315
316 **Comparison with chromatin interaction data**
317 To examine whether the biased orientation of DNA motif sequences is associated
318 with chromatin interactions, enhancer-promoter interactions (EPI) predicted based on

319 enhancer-promoter associations (EPA) were compared with chromatin interaction data
320 (Hi-C). Due to the resolution of Hi-C experimental data used in this study (50kb), EPI
321 were adjusted to 50kb resolution. EPI were predicted based on three types of EPA: (i)
322 EPA shortened at the genomic locations of FR or RF orientation of DNA motif sequence
323 of a TF, (ii) EPA shortened at the genomic locations of DNA motif sequence of a TF
324 acting as insulator sites such as CTCF and cohesin (RAD21, SMC3) without
325 considering their orientation, and (iii) EPA without being shortened by the genomic
326 locations of a DNA motif sequence. EPA (i) showed a significantly higher ratio of EPI
327 overlapped with chromatin interactions (Hi-C) using DNA binding motif sequences of
328 CTCF and cohesin (RAD21 and SMC3) than the other two types of EPAs (n = 4,
329 binomial test, two-sided) (Supplemental Fig. S4). Total 59 biased orientation (40 FR
330 and 23 RF) of DNA motif sequences including CTCF, cohesin, and YY1 showed a
331 significantly higher ratio of EPI overlapped with Hi-C chromatin interactions (a cutoff
332 score of CHiCAGO tool > 1) than the other types of EPAs in monocytes (Supplemental
333 Table S10). When comparing EPI predicted based on only EPA (i) and (iii) with
334 chromatin interactions, total 174 biased orientation (101 FR and 84 RF) of DNA motif
335 sequences showed a significantly higher ratio of EPI predicted based on EPA (i)
336 overlapped with the chromatin interactions than EPI predicted based on EPA (iii)
337 (Supplemental material 2). The difference between EPI predicted based on EPA (i) and
338 (ii) seemed to be difficult to distinguish using the chromatin interaction data and the
339 statistical test in some cases. However, as for the difference between EPI predicted
340 based on EPA (i) and (iii), a larger number of biased orientation of DNA motif

341 sequences was found to be correlated with chromatin interaction data. Chromatin
342 interaction data were obtained from different samples from DNase-seq, open chromatin
343 regions, so individual differences seemed to be large from the results of this analysis.
344 Since, for some DNA motif sequences of transcription factors, the number of EPI
345 overlapped with chromatin interactions was small, if higher resolution of chromatin
346 interaction data (such as HiChIP, in situ DNase Hi-C, and in situ Hi-C data, or a tool to
347 improve the resolution such as HiCPlus) is available, the number of EPI overlapped
348 with chromatin interactions would be increased and the difference of the numbers
349 among three types of EPA would be larger and more significant (Rao et al. 2014;
350 Ramani et al. 2016; Mumbach et al. 2017; Zhang et al. 2018).

351 After the analysis of $CD14^+$ monocytes, to utilize HiChIP chromatin interaction
352 data in $CD4^+$ T cells, the same analysis for $CD14^+$ monocytes was performed using
353 DNase-seq data of four donors in $CD4^+$ T cells (Mumbach et al. 2017). EPI predicted
354 based on EPA were compared with HiChIP chromatin interaction data in $CD4^+$ T cells.
355 The resolutions of HiChIP chromatin interaction data and EPI were adjusted to 5kb. EPI
356 were predicted based on the three types of EPA in the same way as $CD14^+$ monocytes
357 using top 60% of all the transcript (gene) excluding transcripts not expressed in T cells.
358 The criteria of the analysis were determined to include known DNA motif sequences
359 involved in chromatin interactions such as CTCF and cohesin in the result, and the
360 result was consistent with that using Hi-C chromatin interaction data. EPA (iii) showed
361 the highest ratio of EPI overlapped with chromatin interactions (HiChIP) using DNA
362 binding motif sequences of CTCF and cohesin (RAD21 and SMC3), compared with the

363 other two types of EPAs (n = 4, binomial test, two-sided) (Fig. 4). Total 121 biased
364 orientation (73 FR and 58 RF) of DNA motif sequences including CTCF, cohesin,
365 ZNF143, and SMARC showed a significantly higher ratio of EPI overlapped with
366 HiChIP chromatin interactions (more than 1,000 counts for each interaction) than the
367 other types of EPAs in T cells (Table 5). When comparing EPI predicted based on only
368 EPA (i) and (iii) with the chromatin interactions, total 226 biased orientation (132 FR
369 and 123 RF) of DNA motif sequences showed a significantly higher ratio of EPI
370 predicted based on EPA (i) overlapped with the chromatin interactions than EPI
371 predicted based on EPA (iii) (Supplemental material 2). As expected, the number of EPI
372 overlapped with chromatin interactions (HiChIP) was increased, compared with Hi-C
373 chromatin interactions. Most of biased orientation of DNA motif sequences (85%) were
374 found to be correlated with chromatin interactions, when comparing EPI predicted
375 based on EPA (i) and (iii) with HiChIP chromatin interactions.

376 Though the ratios of EPI overlapped with chromatin interactions were increased
377 by using many chromatin interaction data including lower score and count of chromatin
378 interactions (a cutoff score of CHiCAGO tool > 1 for Hi-C and more than 1,000 counts
379 for HiChIP), the ratios of EPI overlapped with chromatin interactions showed the same
380 tendency among the three types of EPAs. The ratio of EPI overlapped with Hi-C
381 chromatin interactions was increased using H3K27ac marks in both monocytes and T
382 cells. The ratio of EPI overlapped with HiChIP chromatin interactions was also
383 increased using H3K27ac marks. Chromatin interaction data were obtained from
384 different samples from DNase-seq, open chromatin regions in $CD4^+$ T cells, so

385 individual differences seemed to be large from the results of this analysis, and
386 (Mumbach et al. 2017) suggested that individual differences of chromatin interactions
387 were larger than those of open chromatin regions. ATAC-seq data, open chromatin
388 regions were available in $CD4^+$ T cells in the paper, however, when using ATAC-seq
389 data, the result of the analysis of biased orientation of DNA motif sequences was
390 different from DNase-seq data, and not included a part of CTCF and cohesin. Thus,
391 DNase-seq data collected from ENCODE and Blueprint projects were employed in this
392 study.
393

394 **Discussion**

395 To find DNA motif sequences of transcription factors (TF) and repeat DNA
396 sequences affecting the expression level of human putative transcriptional target genes,
397 the DNA motif sequences were searched from open chromatin regions of monocytes of
398 four people. Total 287 biased [159 forward-reverse (FR) and 153 reverse-forward (RF)]
399 orientation of DNA motif sequences of TF were found in monocytes of four people in
400 common, whereas only one any orientation (i.e. without considering orientation) of
401 DNA motif sequence of TF was found to affect the expression level of putative
402 transcriptional target genes, suggesting that enhancer-promoter association (EPA)
403 shortened at the genomic locations of FR or RF orientation of the DNA motif sequence
404 of a TF or a repeat DNA sequence is an important character for the prediction of
405 enhancer-promoter interactions (EPI) and the transcriptional regulation of genes.

406 When DNA motif sequences were searched from monocytes of one person, a

407 larger number of biased orientation of DNA motif sequences affecting the expression
408 level of human putative transcriptional target genes were found. When the number of
409 donors, from which experimental data were obtained, was increased, the number of
410 DNA motif sequences found in all people in common decreased and in some cases,
411 known transcription factors involved in chromatin interactions such as CTCF and
412 cohesin (RAD21 and SMC3) were not identified by statistical tests. This would be
413 caused by individual difference of the same cell type, low quality of experimental data,
414 and experimental errors. Moreover, though FR orientation of DNA binding motif
415 sequences of CTCF and cohesin is frequently observed at chromatin interaction anchors,
416 the percentage of FR orientation is not 100, and other orientations of the DNA binding
417 motif sequences are also observed. Though DNA binding motif sequences of CTCF and
418 cohesin are found in various open chromatin regions, DNA binding motif sequences of
419 some TF would be observed less frequently in open chromatin regions. The analyses of
420 experimental data of a number of people would avoid missing relatively weak statistical
421 significance of DNA motif sequences of TF in experimental data of each person by
422 multiple testing correction of thousands of statistical tests. A DNA motif sequence was
423 found with p-value < 0.05 in experimental data of one person and the DNA motif
424 sequence found in the same cell type of four people in common would have p-value $<$
425 $0.05^4 = 6.25 \times 10^{-6}$. Actually, DNA motif sequences with p-value slightly less than 0.05
426 in monocytes of one person were observed in monocytes of four people in common.

427 EPI were compared with chromatin interactions (Hi-C) in monocytes. EPAs
428 shortened at the genomic locations of DNA binding motif sequences of CTCF and

429 cohesin (RAD21 and SMC3) showed a significant difference of the ratios of EPI
430 overlapped with chromatin interactions, according to three types of EPAs (see Methods).
431 Using open chromatin regions overlapped with ChIP-seq experimental data of histone
432 modification of an enhancer mark (H3K27ac), the ratio of EPI not overlapped with
433 Hi-C was reduced. (Phanstiel et al. 2017) also reported that there was an especially
434 strong enrichment for loops with H3K27 acetylation peaks at both ends (Fisher's Exact
435 Test, $p = 1.4 \times 10^{-27}$). However, the total number of EPI overlapped with chromatin
436 interactions was also reduced using H3K27ac peaks, so more chromatin interaction data
437 would be needed to obtain reliable results in this analysis. As an issue of experimental
438 data, data for chromatin interactions and open chromatin regions were came from
439 different samples and donors, so individual differences would exist in the data.
440 Moreover, the resolution of chromatin interaction data used in monocytes was about
441 50kb, thus the number of chromatin interactions was relatively small (72,284 at 50kb
442 resolution with a cutoff score of CHiCAGO tool > 1 and 16,501 with a cutoff score of
443 CHiCAGO tool > 5). EPI predicted based on EPA shortened at the genomic locations of
444 DNA binding motif sequence of TF that were found in various open chromatin regions
445 such as CTCF and cohesin (RAD21 and SMC3) tended to be overlapped with a larger
446 number of chromatin interactions than TF less frequently observed in open chromatin
447 regions. Therefore, to examine the difference of the numbers of EPI overlapped with
448 chromatin interactions, according to the three types of EPAs, the number of chromatin
449 interactions should be large enough.

450 As HiChIP chromatin interaction data were available in $CD4^+$ T cells, biased

451 orientation of DNA motif sequences of TF were examined in T cells using DNase-seq
452 data of four people. The resolutions of chromatin interactions and EPI were adjusted to
453 5kb by fragmentation of genome sequences. In monocytes, the resolution of Hi-C
454 chromatin interaction data was converted by extending anchor regions of chromatin
455 interactions to 50kb length and merging the chromatin interactions overlapped with
456 each other. Fragmentation of genome sequences may affect the classification of
457 chromatin interactions of which anchors are located near the border of a fragment, but
458 the number of chromatin interactions would not be decreased, compared with merging
459 chromatin interactions. The number of HiChIP chromatin interactions was 19,926,360
460 at 5kb resolution, 666,149 at 5kb resolution with chromatin interactions (more than
461 1,000 counts for each interaction), and 78,209 at 5kb resolution with chromatin
462 interactions (more than 6,000 counts for each interaction). As expected, the number of
463 EPI overlapped with chromatin interactions was increased, and 46 – 85% of biased
464 orientation of DNA motif sequences of TF showed a statistical significance in EPI
465 predicted based on EPA shortened at the genomic locations of the DNA motif sequence,
466 compared with the other types of EPAs or EPA not shortened. False positive predictions
467 of EPI would be decreased by using H3K27ac marks and other features. The ratio of
468 EPI overlapped with Hi-C chromatin interactions was increased using H3K27ac marks
469 in both monocytes and T cells. The ratio of EPI overlapped with HiChIP chromatin
470 interactions was also increased using H3K27ac marks. However, the number of biased
471 orientation of DNA motif sequences showing a higher ratio of EPI overlapped with
472 HiChIP chromatin interactions than the other types of EPAs was decreased using

473 H3K27ac marks (Supplemental material 2).

474 Though the number of known DNA binding proteins and TF involved in
475 chromatin interactions would be less than 30 or so, about 300 DNA binding proteins
476 showed enrichment of biased orientation of their DNA binding sequences, and known
477 DNA binding proteins involved in chromatin interactions were found in the biased
478 orientation of DNA binding sequences. JUNDM2 (JDP2) found in T cells and
479 monocytes is not known DNA binding proteins involved in chromatin interactions.
480 JDP2 is involved in histone and nucleosome-related functions such as
481 histone-chaperone activity, promoting nucleosome, and inhibition of histone acetylation
482 (Jin et al. 2006). JDP2 forms a homodimer or heterodimer with various TF
483 (https://en.wikipedia.org/wiki/Jun_dimerization_protein). Thus, the main function of
484 JDP2 may not be associated with chromatin interactions, but it forms a homodimer or
485 heterodimer with TF, potentially forming a chromatin interaction through the binding of
486 JDP2 and another TF, like chromatin interactions formed by YY1 (Weintraub et al.
487 2017). In the analysis of HiChIP chromatin interaction data, JDP2 was in the list of
488 biased orientation of DNA motif sequences showing a higher ratio of EPI overlapped
489 with HiChIP chromatin interactions than the other types of EPAs, using chromatin
490 interactions with more than 6,000 counts for each interaction (Supplemental material 2).
491 When forming a homodimer or heterodimer with another TF, TF may bind to genome
492 DNA with a specific orientation of their DNA binding sequences. From the analysis of
493 biased orientation of DNA motif sequences of TF, TF forming heterodimer would also
494 be found. If the DNA binding motif sequence of only the mate to a pair of TF was found

495 in EPA, EPA was shortened at one side, which is the genomic location of the DNA
496 binding motif sequence of the mate to the pair, and transcriptional target genes were
497 predicted using the EPA shortened at the side. In this analysis, the mate to both
498 heterodimer and homodimer of TF can be used to examine the effect on the expression
499 level of transcriptional target genes predicted based on the EPA shortened at one side.
500 For heterodimer, biased orientation of DNA motif sequences may also be found in
501 forward-forward or reverse-reverse orientation.

502 I reported that the ratio of the number of functional enrichment of putative
503 transcriptional target genes in the total number of putative transcriptional target genes
504 changed according to the types of EPAs, in the same way as gene expression level
505 (Osato 2018). JDP2 showed a higher ratio of functional enrichment of putative
506 transcriptional target genes using EPA shortened at the genomic locations of FR
507 orientation of the DNA binding motif sequence, compared with the other types of EPAs
508 (RF or any orientation) in monocytes and T cells, among monocytes, T cells and $CD20^+$
509 B cells. While the genome-wide analysis of functional enrichment of putative
510 transcriptional target genes takes computational time, the genome-wide analysis of gene
511 expression level is finished with less computational time. The analysis of gene
512 expression level can be used for a cell type and experimental data where the expression
513 levels of transcriptional target genes predicted based on EPA are significantly different
514 from those predicted from only promoter.

515 It has been reported that CTCF and cohesin-binding sites are frequently mutated
516 in cancer (Katainen et al. 2015). Some biased orientation of DNA motif sequences

517 would be associated with chromatin interactions and might be associated with diseases
518 including cancer.
519 The analyses in this study revealed novel characters of DNA binding motif
520 sequences of TF and repeat DNA sequences, and would be useful to analyze TF
521 involved in chromatin interactions and/or forming a homodimer, heterodimer or
522 complex with other TF, affecting the transcriptional regulation of genes.
523

524 ## Methods

525 **Search for biased orientation of DNA motif sequences**

526 To examine transcriptional regulatory target genes of transcription factors (TF),
527 bed files of hg38 of Blueprint DNase-seq data for $CD14^+$ monocytes of four donors
528 (EGAD00001002286; Donor ID: C0010K, C0011I, C001UY, C005PS) were obtained
529 from Blueprint project web site (http://dcc.blueprint-epigenome.eu/#/home), and the bed
530 files of hg38 were converted into those of hg19 using Batch Coordinate Conversion
531 (liftOver) web site (https://genome.ucsc.edu/util.html). Bed files of hg19 of ENCODE
532 H1-hESC (GSM816632; UCSC Accession: wgEncodeEH000556), iPSC (GSM816642;
533 UCSC Accession: wgEncodeEH001110), HUVEC (GSM1014528; UCSC Accession:
534 wgEncodeEH002460), and MCF-7 (GSM816627; UCSC Accession:
535 wgEncodeEH000579) were obtained from the ENCODE websites
536 (http://hgdownload.cse.ucsc.edu/goldenPath/hg19/encodeDCC/wgEncodeUwDgf/;
537 http://hgdownload.cse.ucsc.edu/goldenPath/hg19/encodeDCC/wgEncodeUwDnase/).
538 As high resolution of chromatin interaction data using HiChIP became available

539 in $CD4^+$ T cells, to promote the same analysis of $CD14^+$ monocytes in $CD4^+$ T cells,
540 DNase-seq data of four donors were obtained from a public database and Blueprint
541 projects web sites. DNase-seq data of only one donor was available in Blueprint project
542 for $CD4^+$ T cells (Donor ID: S008H1), and three other DNase-seq data were obtained
543 from NCBI Gene Expression Omnibus (GEO) database. Though the peak calling of
544 DNase-seq data available in GEO database was different from other DNase-seq data in
545 ENCODE and Blueprint projects where 150bp length of peaks were usually predicted
546 using HotSpot (John et al. 2011), FASTQ files of DNase-seq data were downloaded
547 from NCBI Sequence Read Archive (SRA) database (SRR097566, SRR097618, and
548 SRR171574). Read sequences of the FASTQ files were aligned to the hg19 version of
549 the human genome reference using BWA (Li and Durbin 2009), and the BAM files
550 generated by BWA were converted into SAM files, sorted, and indexed using Samtools
551 (Li et al. 2009). Peaks of the DNase-seq data were predicted using HotSpot-4.1.1.

552 To identify transcription factor binding sites (TFBS) from the DNase-seq data,
553 TRANSFAC (2013.2), JASPAR (2010), UniPROBE, BEEML-PBM, high-throughput
554 SELEX, Human Protein-DNA Interactome, and transcription factor binding sequences
555 of ENCODE ChIP-seq data were used (Wingender et al. 1996; Newburger and Bulyk
556 2009; Portales-Casamar et al. 2010; Xie et al. 2010; Zhao and Stormo 2011; Jolma et al.
557 2013; Kheradpour and Kellis 2014). Position weight matrices of transcription factor
558 binding sequences were transformed into TRANSFAC matrices and then into MEME
559 matrices using in-house scripts and transfac2meme in MEME suite (Bailey et al. 2009).
560 Transcription factor binding sequences of TF derived from vertebrates were used for

561 further analyses. Transcription factor binding sequences were searched from each
562 narrow peak of DNase-seq data using FIMO with *p*-value threshold of 10^{-5} (Grant et al.
563 2011). TF corresponding to transcription factor binding sequences were searched
564 computationally by comparing their names and gene symbols of HGNC (HUGO Gene
565 Nomenclature Committee) -approved gene nomenclature and 31,848 UCSC known
566 canonical transcripts
567 (http://hgdownload.cse.ucsc.edu/goldenpath/hg19/database/knownCanonical.txt.gz), as
568 transcription factor binding sequences were not linked to transcript IDs such as UCSC,
569 RefSeq, and Ensembl transcripts.

570 Target genes of a TF were assigned when its TFBS was found in DNase-seq
571 narrow peaks in promoter or extended regions for enhancer-promoter association of
572 genes (EPA). Promoter and extended regions were defined as follows: promoter regions
573 were those that were within distance of ±5 kb from transcriptional start sites (TSS).
574 Promoter and extended regions were defined as per the following association rule,
575 which is the same as that defined in Figure 3A of a previous study (McLean et al. 2010):
576 the single nearest gene association rule, which extends the regulatory domain to the
577 midpoint between the TSS of the gene and that of the nearest gene upstream and
578 downstream without the limitation of extension length. Extended regions for EPA were
579 shortened at the genomic locations of DNA binding sites of a TF that was the closest to
580 a transcriptional start site, and transcriptional target genes were predicted from the
581 shortened enhancer regions using TFBS. Furthermore, promoter and extended regions
582 for EPA were shortened at the genomic locations of forward–reverse (FR) orientation of

583 DNA binding sites of a TF. When forward or reverse orientation of DNA binding sites
584 were continuously located in genome sequences several times, the most external
585 forward–reverse orientation of DNA binding sites were selected. The genomic positions
586 of genes were identified using 'knownGene.txt.gz' file in UCSC bioinformatics sites
587 (Karolchik et al. 2014). The file 'knownCanonical.txt.gz' was also utilized for choosing
588 representative transcripts among various alternate forms for assigning promoter and
589 extended regions for EPA. From the list of transcription factor binding sequences and
590 transcriptional target genes, redundant transcription factor binding sequences were
591 removed by comparing the target genes of a transcription factor binding sequence and
592 its corresponding TF; if identical, one of the transcription factor binding sequences was
593 used. When the number of transcriptional target genes predicted from a transcription
594 factor binding sequence was less than five, the transcription factor binding sequence
595 was omitted.

596 Repeat DNA sequences were searched from the hg19 version of the human
597 reference genome using RepeatMasker (Smit, AFA & Green, P RepeatMasker at
598 http://www.repeatmasker.org) and RepBase RepeatMasker Edition
599 (http://www.girinst.org).

600 For gene expression data, RNA-seq reads mapped onto human hg19 genome
601 sequences were obtained, including ENCODE long RNA-seq reads with poly-A of
602 H1-hESC, iPSC, HUVEC, and MCF-7 (GSM26284, GSM958733, GSM2344099,
603 GSM2344100, GSM958734, and GSM765388), and UCSF-UBC human reference
604 epigenome mapping project RNA-seq reads with poly-A of naive $CD4^+$ T cells

605 (GSM669617). Two replicates were present for H1-hESC, iPSC, HUVEC, and MCF-7,
606 and a single one for $CD4^+$ T cells. RPKMs of the RNA-seq data were calculated using
607 RSeQC (Wang et al. 2012). For monocytes, Blueprint RNA-seq RPKM data
608 (GSE58310, GSE58310_GeneExpression.csv.gz, Monocytes_Day0_RPMI) were used
609 (Saeed et al. 2014). Based on RPKM, UCSC transcripts with expression level among
610 top 30% of all the transcripts were selected in each cell type.

611 The expression level of transcriptional target genes predicted based on EPA
612 shortened at the genomic locations of DNA motif sequence of a TF or a repeat DNA
613 sequence was compared with the expression level of transcriptional target genes
614 predicted from promoter. For each DNA motif sequence shortening EPA, transcriptional
615 target genes were predicted using about 3,000 – 5,000 DNA binding motif sequences of
616 TF, and the expression level of putative transcriptional target genes of each TF was
617 compared between EPA and only promoter using Mann-Whitney test, two-sided
618 (p-value < 0.05). The number of TF showing a significant difference of expression level
619 of putative transcriptional target genes between EPA and promoter was compared
620 among forward-reverse (FR), reverse-forward (RF), and any orientation (i.e. without
621 considering orientation) of a DNA motif sequence shortening EPA using chi-square test
622 (p-value < 0.05). When a DNA motif sequence of a TF or a repeat DNA sequence
623 shortening EPA showed a significant difference of expression level of putative
624 transcriptional target genes among FR, RF, or any orientation in monocytes of four
625 people in common, the DNA motif sequence was listed.

626 Though forward-reverse orientation of DNA binding motif sequences of CTCF

627 and cohesin are frequently observed at chromatin interaction anchors, the percentage of
628 forward-reverse orientation is not 100, and other orientations of the DNA binding motif
629 sequences are also observed. Though DNA binding motif sequences of CTCF and
630 cohesin are found in various open chromatin regions, DNA binding motif sequences of
631 some transcription factors would be observed less frequently in open chromatin regions.
632 The analyses of experimental data of a number of people would avoid missing relatively
633 weak statistical significance of DNA motif sequences in experimental data of each
634 person by multiple testing correction of thousands of statistical tests. A DNA motif
635 sequence was found with p-value < 0.05 in experimental data of one person and the
636 DNA motif sequence found in the same cell type of four people in common would have
637 p-value $< 0.05^4 = 6.25 \times 10^{-6}$.
638
639 **Co-location of biased orientation of DNA motif sequences**
640 Co-location of biased orientation of DNA binding motif sequences of TF was
641 examined. The number of open chromatin regions with the same pair of DNA binding
642 motif sequences was counted, and when the pair of DNA binding motif sequences were
643 enriched with statistical significance (chi-square test, p-value $< 1.0 \times 10^{-10}$), they were
644 listed. For histone modification of an enhancer mark (H3K27ac), bed files of hg38 of
645 Blueprint ChIP-seq data for $CD14^+$ monocytes (EGAD00001001179) and $CD4^+$ T cells
646 (Donor ID: S000RD) were obtained from Blueprint web site
647 (http://dcc.blueprint-epigenome.eu/#/home), and the bed files of hg38 were converted
648 into those of hg19 using Batch Coordinate Conversion (liftOver) web site

649 (https://genome.ucsc.edu/util.html). Networks of co-locations of biased orientation of
650 DNA motif sequences were plotted using Cytoscape v3.71 with yFiles Layout
651 Algorithms for Cytoscape (Shannon et al. 2003).
652
653 **Comparison with chromatin interaction data**
654 For comparison of EPA in monocytes with chromatin interactions,
655 'PCHiC_peak_matrix_cutoff0.txt.gz' file was downloaded from 'Promoter Capture
656 Hi-C in 17 human primary blood cell types' web site (https://osf.io/u8tzp/files/), and
657 chromatin interactions for Monocytes with scores of CHiCAGO tool > 1 and
658 CHiCAGO tool > 5 were extracted from the file (Javierre et al. 2016). In the same way
659 as monocytes, Hi-C chromatin interaction data of $CD4^+$ T cells (Naive $CD4^+$ T cells,
660 nCD4) were obtained.
661 Enhancer-promoter interactions (EPI) were predicted using three types of EPAs in
662 monocytes: (i) EPA shortened at the genomic locations of FR or RF orientation of DNA
663 motif sequence of a TF, (ii) EPA shortened at the genomic locations of any orientation
664 (i.e. without considering orientation) of DNA motif sequence of a TF, and (iii) EPA
665 without being shortened by a DNA motif sequence. EPI predicted using the three types
666 of EPAs in common were removed. First, EPI predicted based on EPA (i) were
667 compared with chromatin interactions (Hi-C). The resolution of chromatin interaction
668 data used in this study was 50kb, so EPI were adjusted to 50kb before their comparison.
669 The number and ratio of EPI overlapped with chromatin interactions were counted.
670 Second, EPI were predicted based on EPA (ii), and EPI predicted based on EPA (i) were

removed from the EPI. The number and ratio of EPI overlapped with chromatin interactions were counted. Third, EPI were predicted based on EPA (iii), and EPI predicted based on EPA (i) and (ii) were removed from the EPI. The number and ratio of EPI overlapped with chromatin interactions were counted. The number and ratio of the EPI were compared two times between EPA (i) and (iii), and EPA (i) and (ii) (binomial distribution, p-value < 0.025 for each test, two-sided, 95% confidence interval).

For comparison of EPA with chromatin interactions (HiChIP) in $CD4^+$ T cells, 'GSM2705049_Naive_HiChIP_H3K27ac_B2T1_allValidPairs.txt' file was downloaded from Gene Expression Omnibus (GEO) database (GSM2705049). The resolutions of chromatin interaction data and EPI were adjusted to 5kb before their comparison. Chromatin interactions with more than 6,000 and 1,000 counts for each interaction were used in this study.

Acknowledgements

The supercomputing resource was provided by Human Genome Center of the Institute of Medical Science at the University of Tokyo. Computations were partially performed on the NIG supercomputer at ROIS National Institute of Genetics. Publication charges for this article were funded by JSPS KAKENHI Grant Number 16K00387. This research was partially supported by the Platform Project for Supporting in Drug Discovery and Life Science Research（Platform for Dynamic Approaches to Living System）from Japan Agency for Medical Research and Development (AMED). This research was partially supported by Development of Fundamental Technologies for

693 Diagnosis and Therapy Based upon Epigenome Analysis from Japan Agency for
694 Medical Research and Development (AMED). This work was partially supported by
695 JST CREST Grant Number JPMJCR15G1, Japan.
696

697 **Figures**

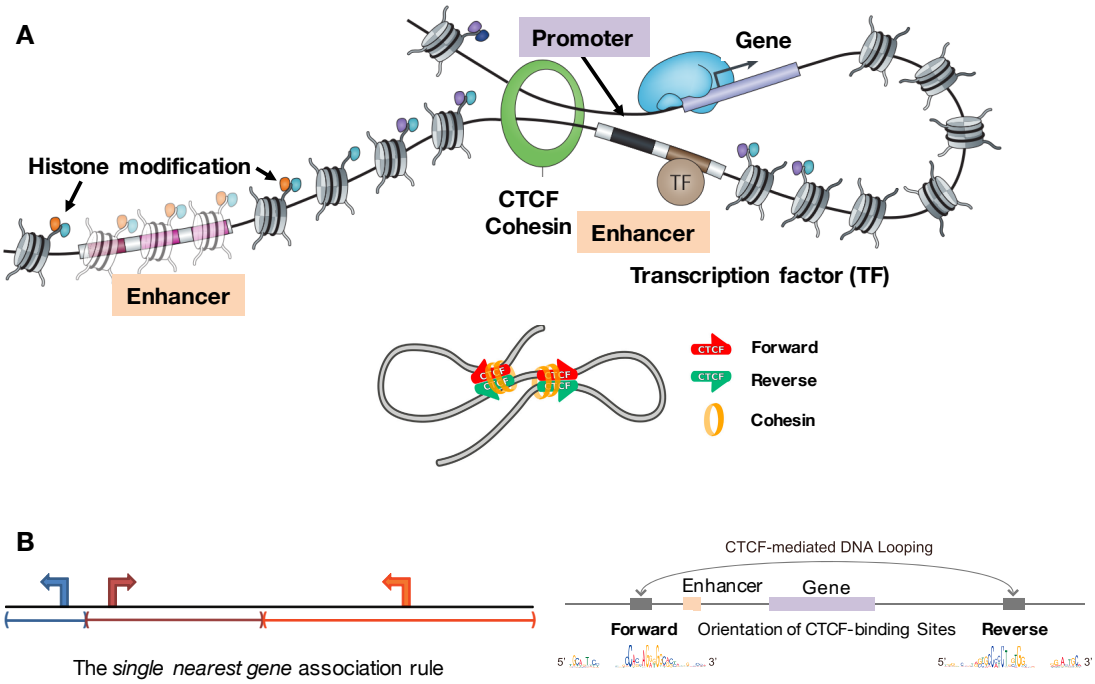

698

699 **Figure 1.** Chromatin interactions and enhancer-promoter association. (A) Forward–
700 reverse orientation of CTCF-binding sites are frequently found in chromatin interaction
701 anchors. CTCF can block the interaction between enhancers and promoters limiting the
702 activity of enhancers to certain functional domains (de Wit et al. 2015; Guo et al. 2015).
703 (B) Computationally-defined regulatory domains for enhancer-promoter association
704 (McLean et al. 2010). The *single nearest gene* association rule extends the regulatory
705 domain to the midpoint between this gene's TSS and the nearest gene's TSS both
706 upstream and downstream. Enhancer-promoter association was shortened at the
707 genomic locations of forward-reverse orientation of DNA binding motif sequence of a
708 transcription factor (e.g. CTCF in the figure).

709

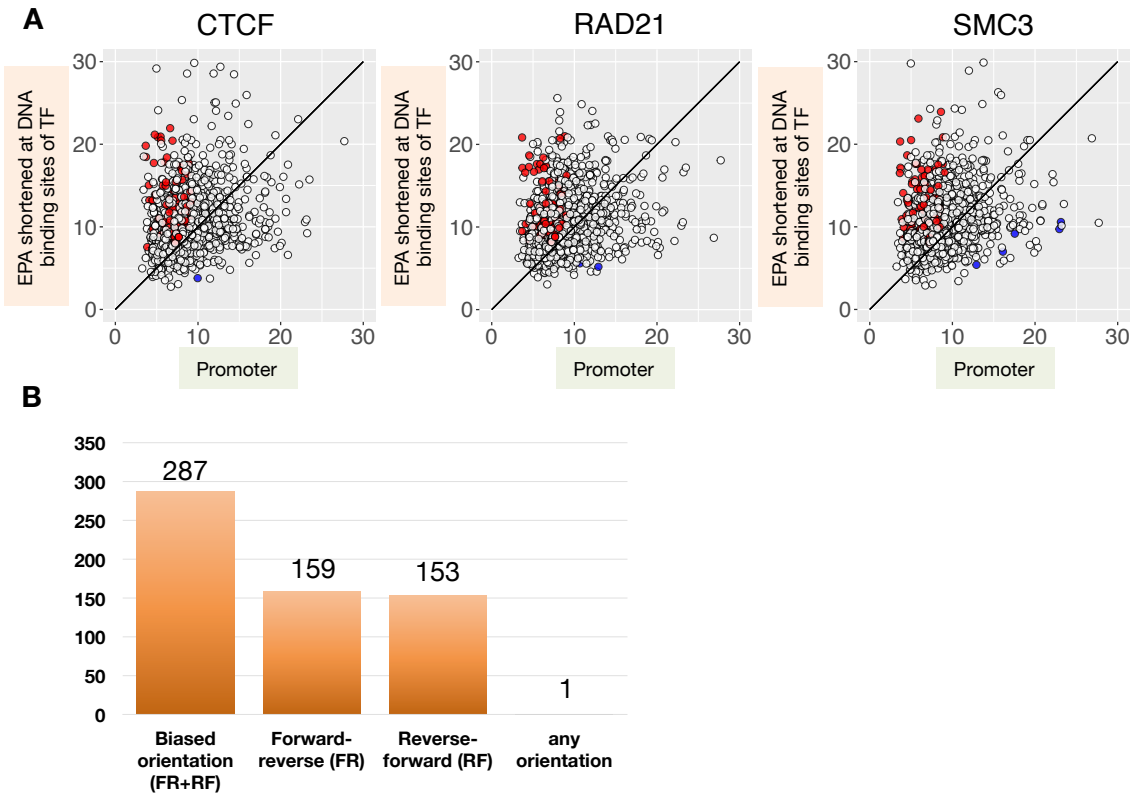

Figure 2. Biased orientation of DNA motif sequences of transcription factors affecting the transcription of genes. (A) Comparison of expression level of putative transcriptional target genes. The median expression levels of target genes of the same transcription factor binding sequences were compared between promoters and enhancer-promoter association (EPA) shortened at the genomic locations of forward-reverse orientation of DNA motif sequence of CTCF and cohesin (RAD21 and SMC3) respectively in monocytes. Red and blue dots show statistically significant difference (Mann-Whitney test) of the distribution of expression levels of target genes between promoters and the EPA. Red dots show the median expression level of target genes was higher based on the EPA than promoters, and blue dots show the median expression level of target genes was lower based on the EPA than promoters. The

722 expression level of target genes predicted based on the EPA tended to be higher than
723 promoters, implying that transcription factors acted as activators of target genes. (B)
724 Biased orientation of DNA motif sequences of transcription factors in monocytes. Total
725 287 of biased orientation of DNA binding motif sequences of transcription factors were
726 found to affect the expression level of putative transcriptional target genes in monocytes
727 of four people in common, whereas only one any orientation (i.e. without considering
728 orientation) of DNA binding motif sequence was found to affect the expression level.
729

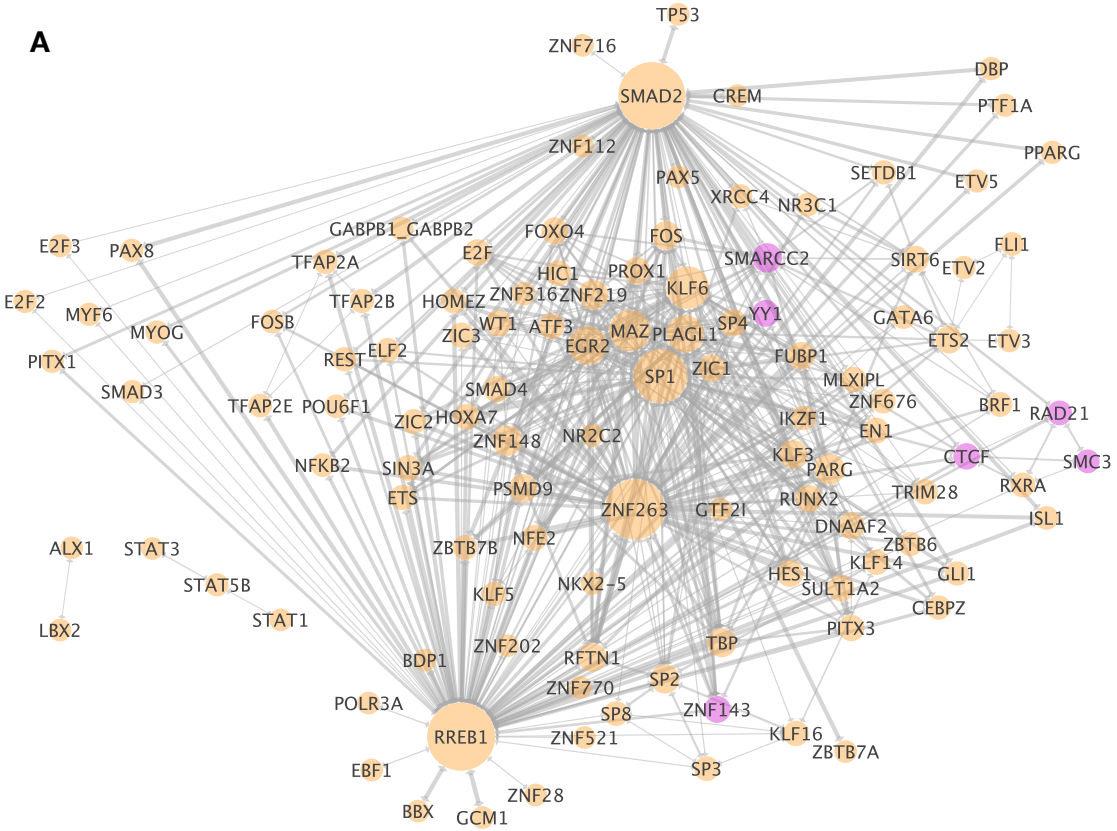

730
731

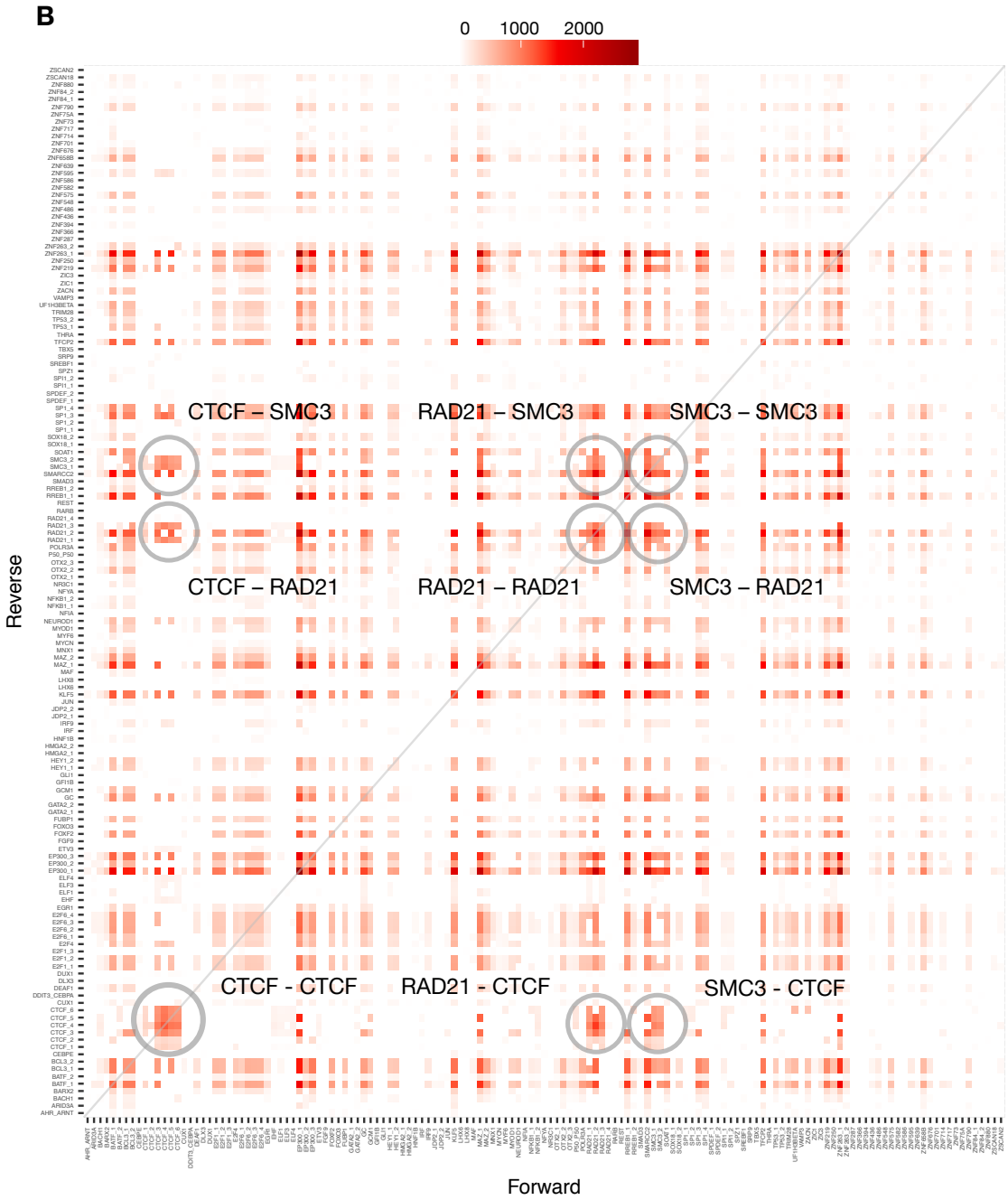

732

733 **Figure 3.** Association of biased orientation of DNA binding motif sequences of

734 transcription factors. (A) Co-location of biased orientation of DNA binding motif

735 sequences of transcription factors. Co-locations of the DNA motif sequences in open

736 chromatin regions were examined in monocytes. When the same DNA motif sequence

737 of a TF was co-localized with DNA motif sequences of more than one TF in the same or
738 different open chromatin regions, these co-locations of DNA motif sequences were
739 connected to each other. Purple circles of TFs are known to be involved in chromatin
740 interactions. The line thickness is correlated with the number of open chromatin regions
741 with co-location of the same pair of DNA motif sequences. The size of a circle is
742 correlated with the number of unique TF co-localized with the TF of the circle, which is
743 the number of edges of the node. (B) Pairs of biased orientation of DNA binding motif
744 sequences of transcription factors enriched in upstream and downstream of genes. The
745 number of genes with a pair of forward-reverse orientation of DNA motif sequences
746 was counted using all pairs of the DNA motif sequences found in open chromatin
747 regions overlapped with H3K27ac histone modification marks in T cells, and statistical
748 tests (chi-square test) were conducted. The number of genes where a pair of
749 forward-reverse orientation of DNA motif sequences were enriched with p-value < 0.05
750 was counted and shown as heat map. Gray circles show pairs of DNA motif sequences
751 of CTCF and cohesin (RAD21 and SMC3). CTCF and cohesin are known to be
752 involved in chromatin interactions and have biased orientation of DNA binding motif
753 sequences to form chromatin loops. Other pairs of forward-reverse orientation of DNA
754 motif sequences were also enriched in upstream and downstream of genes.
755

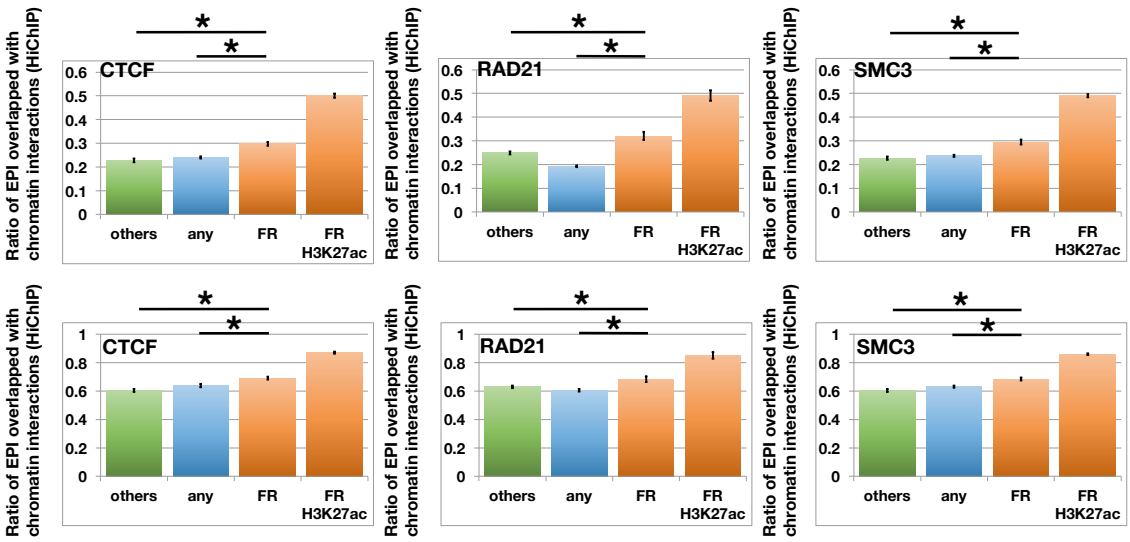

Figure 4. Comparison of enhancer-promoter interactions (EPI) with chromatin interactions in T cells. EPI were predicted based on enhancer-promoter association (EPA) shortened at the genomic locations of biased orientation of DNA binding motif sequence of a transcription factor. Total 121 biased orientation (73 FR and 58 RF) of DNA motif sequences including CTCF and cohesin showed a significantly higher ratio of EPI overlapped with HiChIP chromatin interactions than the other types of EPAs in T cells. The upper part of the figure is a comparison of EPI with HiChIP chromatin interactions with more than 6,000 counts for each interaction, and the lower part of the figure is a comparison of EPI with HiChIP chromatin interactions with more than 1,000 counts for each interaction. FR: forward-reverse orientation of DNA motif. any: any orientation (i.e. without considering orientation) of DNA motif. others: enhancer-promoter association not shortened at the genomic locations of DNA motif. FR H3K27ac: EPI were predicted using DNA motif in open chromatin regions overlapped with H3K27ac histone modification marks. * p-value < 10^{-4}.

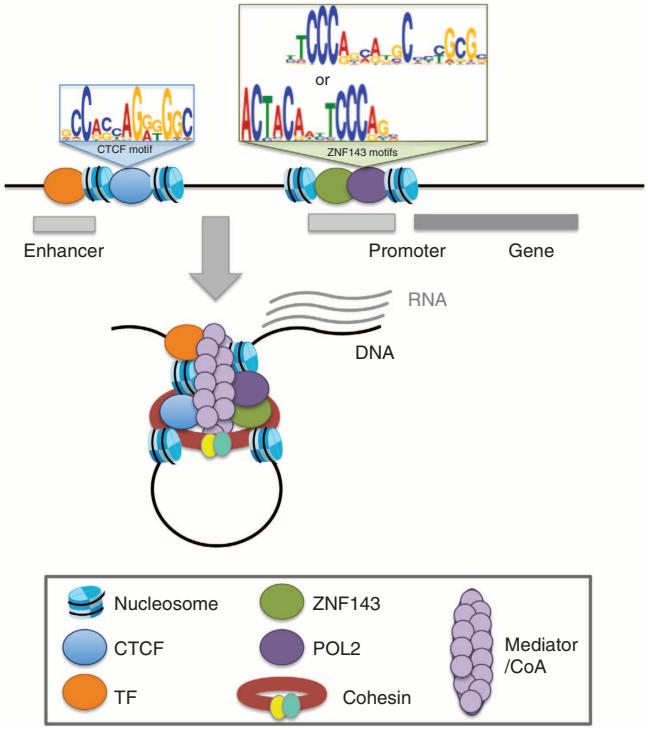

Figure 5. Schematic representation of chromatin interactions involving gene promoters. ZNF143 contributes the formation of chromatin interactions by directly binding the promoter of genes establishing looping with distal element bound by CTCF (Bailey et al. 2015).

Tables

Table 1. Top 90 biased orientation of DNA binding motif sequences of transcription factors in monocytes. TF: DNA binding motif sequences of transcription factors. Score: $-\log_{10}$ (p-value).

Forward-reverse orientation

DNA motif of TF	Score	TF	Score	TF	Score
SRF	75.45	STAT5A	31.24	SMARCC2	21.86
IRF7	71.05	E2F8	30.62	ZNF695	21.78
MINI20	61.68	TP53	30.56	ZNF28	21.77
CTCF	61.62	STAT5B	29.94	ZNF316	21.66
E2F	59.32	STAT3	29.85	TBP	21.60
STAT1	58.94	FOS	29.75	NFIB	21.45
ZNF317	55.97	CEBPZ	29.42	PHOX2B	20.82
CEBPG	55.46	RAD21	28.67	DEC	20.62
ZNF623	54.71	SMAD2	28.60	ZNF709	20.58
ZNF93	54.23	GATA2	28.52	YY1	20.57
HMBOX1	52.99	KLF6	28.02	EIF5A2	20.55
SMAD2_SMAD3_SMAD4	50.66	HOXB1	27.62	ZNF148	20.45
FOXN2	49.88	GLI1	27.09	PAX5	20.05
SPEF1	49.52	GCM1	26.73	POU6F1	19.93
ZNF646	43.95	ZNF676	26.66	FOXO4	19.72
TFE3	42.46	TCF3	26.32	EBF	19.26
MYB	41.98	EHF	26.32	ZNF648	19.12
STAT4	40.54	TCF12	26.29	HENMT1	19.02
ZNF716	40.39	MEF2A	26.22	PARG	18.78
KLF14	39.64	HIC1	25.34	ZNF460	18.64
FOXA1	38.13	EGR2	24.92	SLC25A20	17.83
USF	37.74	NR2F2	24.86	KLF5	17.77
EN1	37.01	PLAGL1	24.65	XRCC4	17.53
ZNF219	35.37	REST	24.53	WT1	17.34
IKZF1	33.79	ZNF143	23.67	SULT1A2	17.34
ZIC1	33.60	YBX1	22.99	FUBP1	17.33
SMC3	33.37	PRDM15	22.63	DNAAF2	17.26
ESR2	32.07	ZNF92	22.22	ZNF521	17.25
TP63	31.98	ZNF214	22.11	XBP1	16.85
ZNF836	31.66	PTF1A	22.09	SP1	16.84

Reverse-forward orientation

TF	Score	TF	Score	TF	Score
RFX5	102.30	TFAP2B	34.55	ZNF449	27.96
TCF7	75.34	TBP	34.47	ZNF233	27.66
SRF	65.52	ZNF670	34.33	SOX2	26.46
ZNF28	63.89	ZNF350	34.30	RXRA	26.07
HNF1B	62.46	ZNF687	33.82	MYF6	25.85
ZNF225	62.18	NFKB2	33.05	MAFK	25.81
CEBPB	59.69	RFX3	32.74	CEBPZ	25.73
NFY	58.96	NFE2L3	32.69	POU2F2	25.59
ZNF286B	54.73	TRIM28	32.27	ETS2	25.05
CTCF	53.16	SP3	32.22	HSF1	24.76
PAX5	52.57	FLI1	32.15	AHR	23.56
STAT1	52.11	RBAK	31.92	PAX6	23.48
ISL1	49.73	NR2F1	31.80	IRF4	22.47
ETV7	47.08	NKX3-1	31.55	ETV3	21.90
KLF16	46.45	ZIC2	31.40	FOXP2	21.72
SP1	46.03	PARP1	31.19	CDX2	21.45
SMAD3	45.27	ZNF195	31.06	NFATC1	21.24
STAT5B	44.72	BDP1	30.84	SP4	21.14
TEAD1	43.00	SOX9	30.72	USF1	20.92
ZNF579	42.94	SP8	30.49	MSX2	20.84
ZBTB2	42.28	ZNF121	30.04	PPARG	20.70
ZNF343	41.01	ZNF202	30.01	MYEF2	20.23
DOBOX5	39.21	CD59	29.85	MYC_MAX	20.22
NANOG	38.84	RXRB	29.57	ZNF711	19.84
NFE2L2	38.53	STAT5A	29.31	ZBTB18	19.60
OBOX2	38.00	SOX11	29.09	HSF2	19.51
ZNF652	37.84	WT1	29.06	DNAAF2	19.00
ZNF30	37.59	CREM	28.65	IRF3	18.88
MYOG	36.34	ZNF316	28.34	TFAP2E	18.87
GABPB1_GABPB2	35.96	HAND1_TCF3	28.07	BCL11A	18.59

Table 2. Top 30 forward-reverse orientation of DNA binding motif sequences of transcription factors in MCF-7 and iPS cells. TF: DNA binding motif sequences of transcription factors. Score: $-\log_{10}$ (p-value).

MCF-7

TF	Score
RAD21	16.21
SMC3	15.63
CTCF	15.12
E2F	10.14
SLC25A20	9.62
HOXA7	8.29
STAT5B	7.55
REST	7.25
SIRT6	7.05
KLF3	6.53
YY1	5.30
PLAGL1	4.97
ZNF219	4.91
STAT1	4.43
SNTB1	4.42
ETS	3.16
XRCC4	3.15
ZBTB6	3.12
DBP	2.53
SETDB1	2.53
RREB1	2.50
E2F5	2.38
KLF5	2.33
SPEF1	2.22
ZNF143	2.20
ZNF460	2.19
FOS	2.18
GATA2	1.97
MAZ	1.95
PARG	1.94

iPS

TF	Score
ZIC3	19.32
ZNF521	18.93
TFE3	16.63
ZNF317	16.43
NKX2-5	16.25
HES1	15.34
ZBTB24	14.21
SMC3	13.76
FOS	13.69
RAD21	13.05
ZNF836	11.64
TBX5	11.48
CTCF	11.24
STAT1	11.19
RUNX2	10.28
WT1	10.27
ZIC1	9.60
MAX	8.55
KLF3	8.29
KLF14	8.25
ZNF143	7.81
E2F5	7.66
SIRT6	7.56
EN1	7.49
YY1	7.02
STAT5B	6.73
MAZ	6.39
ZNF148	6.20
TCF3	5.73
EGR2	5.45

Table 3. Biased orientation of repeat DNA sequences in monocytes. Score: $-\log_{10}$ (p-value).

Forward-reverse (FR) orientation (using H3K27ac histone modification marks)

Repeat DNA seq.	Score
MLT1F1	6.75

Reverse-forward (RF) orientation

Repeat DNA seq.	Score
LTR16C	69.39
L1ME4b	23.90
AluSg	23.61

Table 4. Top 30 of co-locations of biased orientation of DNA binding motif sequences of transcription factors in monocytes. Co-locations of DNA motif sequence of CTCF with another biased orientation of DNA motif sequence were shown in a separate table. Motif 1,2: DNA binding motif sequences of transcription factors. # both: the number of open chromatin regions including both Motif 1 and Motif 2. # motif 1: the number of open chromatin regions including Motif 1. # motif 2: the number of open chromatin regions including Motif 2. # others: the number of open chromatin regions not including Motif 1 and Motif 2. Open chromatin regions overlapped with histone modification marks (H3K27ac) were used (Total 26,095 regions).

Motif 1	Motif 2	# both	# motif 1	# motif 2	# others	*p*-value
CTCF	SMAD2	4527	781	4478	16309	0
CTCF	RREB1	4379	929	4757	16030	0
CTCF	ZNF263	4357	951	4875	15912	0
CTCF	SP1	4321	987	4052	16735	0
CTCF	RAD21	3804	1504	225	20562	0
CTCF	KLF6	3695	852	3800	17748	0
CTCF	SMC3	1259	178	1977	22681	0
CTCF	RXRA	1220	259	2559	22057	0

Motif 1	Motif 2	# both	# motif 1	# motif 2	# others	*p*-value
SMAD2	ZNF263	7427	1578	1805	15285	0
SMARCC2	ZNF263	7354	1192	1893	15656	0
RREB1	SP1	7208	1957	1165	15765	0
SIRT6	ZNF263	7126	1154	2121	15694	0
MAZ	SP1	7052	909	1321	16813	0
MAZ	ZNF263	7022	999	2225	15849	0
SP1	ZNF263	7009	1364	2223	15499	0
SMAD2	SP1	6925	2080	1448	15642	0
MAZ	RREB1	6920	967	2245	15963	0
SIRT6	SMAD2	6766	1514	2239	15576	0
SIRT6	SMARCC2	6668	1612	1878	15937	0
PLAGL1	SMAD2	6637	1074	2368	16016	0
MAZ	SMAD2	6627	1334	2378	15756	0
PARG	SMAD2	6602	1012	2403	16078	0
PLAGL1	ZNF263	6571	1140	2661	15723	0
EGR2	RREB1	6565	787	2600	16143	0
KLF6	RREB1	6563	932	2573	16027	0
MAZ	SMARCC2	6562	1459	1984	16090	0
RREB1	ZNF263	6551	1607	2681	15256	0
KLF6	SP1	6541	954	1832	16768	0
PLAGL1	RREB1	6496	1215	2640	15744	0
EGR2	SP1	6492	860	1881	16862	0
KLF6	SMAD2	6491	1004	2514	16086	0
PARG	ZNF263	6390	1224	2842	15639	0
PLAGL1	SP1	6318	1393	2055	16329	0
KLF6	ZNF263	6304	1191	2928	15672	0
EGR2	SMAD2	6270	1082	2735	16008	0
EGR2	ZNF263	6253	1099	2979	15764	0
EGR2	MAZ	6219	1133	1742	17001	0
PARG	RREB1	6219	1395	2917	15564	0

809 **Table 5.** Comparison of enhancer-promoter interactions (EPI) with chromatin
810 interactions in T cells. TF: DNA binding motif sequence of a transcription factor. Score:
811 $-\log_{10}$ (*p*-value). Inf: *p*-value = 0. Score 1: Comparison of EPA shortened at the
812 genomic locations of FR or RF orientation of DNA motif sequence with EPA not
813 shortened. Score 2: Comparison of EPA shortened at the genomic locations of FR or RF
814 orientation of DNA motif sequence with EPA shortened at the genomic locations of any
815 orientation of DNA motif sequence.

816

817 Forward-reverse (FR) orientation

TF	Score 1	Score 2
APEX1	13.57	3.85
AR	Inf	8.30
CDC5L	65.46	12.23
CTCF	101.79	14.94
DDIT3_CEBPA	249.72	4.78
EBF1	48.10	2.27
EGR1	97.56	6.09
EGR3	130.86	2.73
EGR4	59.94	2.91
ELF5	119.97	2.85
EP300	28.41	15.12
ETV4	270.06	2.16
FOXF2	42.79	5.16
FOXN4	76.81	4.80
FOXO3	323.31	5.49
FOXO6	63.29	1.77
GATA	104.41	2.17
GATA5	89.03	4.38
GFI1B	184.13	11.81
GLIS2	32.14	1.87
HBP1	281.23	3.05
HIC1	101.63	3.27
HOXA13	103.63	3.71
HOXA2	323.31	5.81
INSM2	323.31	2.02
IRF	206.25	2.09
IRF5	39.54	3.78
KLF1	146.64	3.51
LHX8	245.03	2.34
MAF	66.63	3.85
MINI20	102.68	3.29
MYC	39.24	2.64
MZF1	24.10	1.64
NFATC2	37.81	1.92
NFKB1	195.32	11.43
NR0B1	13.24	1.84
NR2C2	137.27	12.28
OTX2	40.38	2.77
P50_P50	131.79	6.49
PITX1	37.22	2.17

TF	Score 1	Score 2
PRDM15	Inf	3.21
RAD21	56.16	4.21
RARB	113.99	2.28
REL	104.66	7.95
RREB	117.64	3.13
RREB1	116.79	3.39
SMC3	90.56	17.59
SOAT1	22.63	1.88
SOX18	113.13	6.71
SRP9	117.49	3.47
TAL1	70.39	1.82
TCF7L2	93.32	8.22
TFCP2	260.99	4.13
THRA	145.85	4.05
TP53	323.31	9.13
TP63	172.00	3.90
YBX1	164.76	5.23
ZBTB7A	66.49	4.74
ZFP14	97.38	5.25
ZNF219	32.59	7.48
ZNF253	323.31	21.30
ZNF585A	185.37	6.09
ZNF616	129.96	8.66
ZNF639	193.43	1.77
ZNF681	323.31	35.04
ZNF701	41.48	1.65
ZNF721	225.60	5.52
ZNF75A	43.99	3.51
ZNF770	66.18	2.95
ZNF786	323.31	15.68
ZNF790	74.59	6.71
ZNF84	149.37	3.38
ZNF846	Inf	10.92

Reverse-forward (RF) orientation

TF	Score 1	Score 2
BCL11B	101.77	5.58
CEBPA	323.31	2.37
CREB3	139.16	13.51
CTCF	119.43	20.80
DBP	25.72	1.84
EGR1	247.74	1.65
EP300	135.93	6.30
ESR1	101.75	9.30
ETS1	250.92	1.76
ETV1	272.94	3.43
ETV3	323.31	2.99
FOS	101.53	9.02
FOXA	323.31	9.16
FOXA1	323.31	8.99
FOXG1	235.13	2.77
FOXN4	61.07	5.39
FOXO3	306.90	5.33
GATA1	314.93	1.91
HLTF	82.82	1.85
HOXA10	29.26	1.81
HOXB6	197.15	2.21
IRF5	Inf	6.92
KLF13	148.08	4.91
KLF8	120.36	2.97
NFE2L2	155.83	3.83
NFKB1	106.02	7.09
NKX2-1	323.31	4.01
NKX2-4	Inf	5.73
NKX2-5	323.31	5.80
NR4A1	116.75	2.99
PPARGC1A	57.39	3.36
RAD21	41.87	3.16
RUNX2	124.18	5.84
SIX6	95.00	3.28
SMARC	323.31	6.02
SRF	323.31	6.78
TAL1	124.35	4.80
TCF12	74.48	2.21
ZBTB18	240.63	9.05
ZBTB4	323.31	2.06

TF	Score 1	Score 2
ZFP2	323.31	6.24
ZNF143	134.24	1.81
ZNF174	159.72	7.65
ZNF257	172.88	3.75
ZNF28	323.31	3.53
ZNF282	100.44	4.02
ZNF300	Inf	3.91
ZNF341	94.91	5.59
ZNF44	165.34	3.45
ZNF484	301.75	12.63
ZNF526	82.28	4.67
ZNF580	55.73	2.98
ZNF625	323.31	2.31
ZNF658	92.95	4.92
ZNF718	165.94	2.09
ZNF721	86.39	7.28
ZNF773	219.31	13.43
ZNF777	137.69	1.96

818

819 **References**

820

821 Bailey SD, Zhang X, Desai K, Aid M, Corradin O, Cowper-Sal Lari R, Akhtar-Zaidi B,
822 Scacheri PC, Haibe-Kains B, Lupien M. 2015. ZNF143 provides sequence
823 specificity to secure chromatin interactions at gene promoters. *Nat Commun* **2**:
824 6186.
825 Bailey TL, Boden M, Buske FA, Frith M, Grant CE, Clementi L, Ren J, Li WW, Noble
826 WS. 2009. MEME SUITE: tools for motif discovery and searching. *Nucleic*
827 *acids research* **37**: W202-208.
828 Barutcu AR, Lajoie BR, Fritz AJ, McCord RP, Nickerson JA, van Wijnen AJ, Lian JB,
829 Stein JL, Dekker J, Stein GS et al. 2016. SMARCA4 regulates gene expression
830 and higher-order chromatin structure in proliferating mammary epithelial cells.
831 *Genome research* **26**: 1188-1201.
832 Bejerano G, Lowe CB, Ahituv N, King B, Siepel A, Salama SR, Rubin EM, Kent WJ,
833 Haussler D. 2006. A distal enhancer and an ultraconserved exon are derived
834 from a novel retroposon. *Nature* **441**: 87-90.
835 Chen M, Manley JL. 2009. Mechanisms of alternative splicing regulation: insights from
836 molecular and genomics approaches. *Nat Rev Mol Cell Biol* **10**: 741-754.
837 Das D, Clark TA, Schweitzer A, Yamamoto M, Marr H, Arribere J, Minovitsky S,
838 Poliakov A, Dubchak I, Blume JE et al. 2007. A correlation with exon
839 expression approach to identify cis-regulatory elements for tissue-specific
840 alternative splicing. *Nucleic acids research* **35**: 4845-4857.
841 de Souza FS, Franchini LF, Rubinstein M. 2013. Exaptation of transposable elements
842 into novel cis-regulatory elements: is the evidence always strong? *Mol Biol Evol*
843 **30**: 1239-1251.
844 de Wit E, Vos ES, Holwerda SJ, Valdes-Quezada C, Verstegen MJ, Teunissen H,
845 Splinter E, Wijchers PJ, Krijger PH, de Laat W. 2015. CTCF Binding Polarity
846 Determines Chromatin Looping. *Molecular cell* **60**: 676-684.
847 Grant CE, Bailey TL, Noble WS. 2011. FIMO: scanning for occurrences of a given
848 motif. *Bioinformatics (Oxford, England)* **27**: 1017-1018.
849 Guo Y, Xu Q, Canzio D, Shou J, Li J, Gorkin DU, Jung I, Wu H, Zhai Y, Tang Y et al.
850 2015. CRISPR Inversion of CTCF Sites Alters Genome Topology and

851 Enhancer/Promoter Function. *Cell* **162**: 900-910.
852 Javierre BM, Burren OS, Wilder SP, Kreuzhuber R, Hill SM, Sewitz S, Cairns J,
853 Wingett SW, Varnai C, Thiecke MJ et al. 2016. Lineage-Specific Genome
854 Architecture Links Enhancers and Non-coding Disease Variants to Target Gene
855 Promoters. *Cell* **167**: 1369-1384 e1319.
856 Jeong M, Huang X, Zhang X, Su J, Shamim M, Bochkov I, Reyes J, Jung H, Heikamp
857 E, Presser Aiden A et al. 2017. A Cell Type-Specific Class of Chromatin Loops
858 Anchored at Large DNA Methylation Nadirs. *bioRxiv*.
859 Ji X, Dadon DB, Abraham BJ, Lee TI, Jaenisch R, Bradner JE, Young RA. 2015.
860 Chromatin proteomic profiling reveals novel proteins associated with
861 histone-marked genomic regions. *Proc Natl Acad Sci U S A* **112**: 3841-3846.
862 Jin C, Kato K, Chimura T, Yamasaki T, Nakade K, Murata T, Li H, Pan J, Zhao M, Sun
863 K et al. 2006. Regulation of histone acetylation and nucleosome assembly by
864 transcription factor JDP2. *Nat Struct Mol Biol* **13**: 331-338.
865 Jjingo D, Conley AB, Wang J, Marino-Ramirez L, Lunyak VV, Jordan IK. 2014.
866 Mammalian-wide interspersed repeat (MIR)-derived enhancers and the
867 regulation of human gene expression. *Mob DNA* **5**: 14.
868 John S, Sabo PJ, Thurman RE, Sung MH, Biddie SC, Johnson TA, Hager GL,
869 Stamatoyannopoulos JA. 2011. Chromatin accessibility pre-determines
870 glucocorticoid receptor binding patterns. *Nature genetics* **43**: 264-268.
871 Jolma A, Yan J, Whitington T, Toivonen J, Nitta KR, Rastas P, Morgunova E, Enge M,
872 Taipale M, Wei G et al. 2013. DNA-binding specificities of human transcription
873 factors. *Cell* **152**: 327-339.
874 Karolchik D, Barber GP, Casper J, Clawson H, Cline MS, Diekhans M, Dreszer TR,
875 Fujita PA, Guruvadoo L, Haeussler M et al. 2014. The UCSC Genome Browser
876 database: 2014 update. *Nucleic acids research* **42**: D764-770.
877 Katainen R, Dave K, Pitkanen E, Palin K, Kivioja T, Valimaki N, Gylfe AE, Ristolainen
878 H, Hanninen UA, Cajuso T et al. 2015. CTCF/cohesin-binding sites are
879 frequently mutated in cancer. *Nature genetics* **47**: 818-821.
880 Kheradpour P, Kellis M. 2014. Systematic discovery and characterization of regulatory
881 motifs in ENCODE TF binding experiments. *Nucleic acids research* **42**:
882 2976-2987.
883 Li H, Durbin R. 2009. Fast and accurate short read alignment with Burrows-Wheeler

884 transform. *Bioinformatics (Oxford, England)* **25**: 1754-1760.
885 Li H, Handsaker B, Wysoker A, Fennell T, Ruan J, Homer N, Marth G, Abecasis G,
886 Durbin R, Genome Project Data Processing S. 2009. The Sequence
887 Alignment/Map format and SAMtools. *Bioinformatics (Oxford, England)* **25**:
888 2078-2079.
889 McLean CY, Bristor D, Hiller M, Clarke SL, Schaar BT, Lowe CB, Wenger AM,
890 Bejerano G. 2010. GREAT improves functional interpretation of cis-regulatory
891 regions. *Nature biotechnology* **28**: 495-501.
892 Mumbach MR, Satpathy AT, Boyle EA, Dai C, Gowen BG, Cho SW, Nguyen ML,
893 Rubin AJ, Granja JM, Kazane KR et al. 2017. Enhancer connectome in primary
894 human cells identifies target genes of disease-associated DNA elements. *Nature*
895 *genetics* **49**: 1602-1612.
896 Newburger DE, Bulyk ML. 2009. UniPROBE: an online database of protein binding
897 microarray data on protein-DNA interactions. *Nucleic acids research* **37**:
898 D77-82.
899 Osato N. 2018. Characteristics of functional enrichment and gene expression level of
900 human putative transcriptional target genes. *BMC Genomics* **19**: 957.
901 Phanstiel DH, Van Bortle K, Spacek D, Hess GT, Shamim MS, Machol I, Love MI,
902 Aiden EL, Bassik MC, Snyder MP. 2017. Static and Dynamic DNA Loops form
903 AP-1-Bound Activation Hubs during Macrophage Development. *Molecular cell*
904 **67**: 1037-1048.e1036.
905 Portales-Casamar E, Thongjuea S, Kwon AT, Arenillas D, Zhao X, Valen E, Yusuf D,
906 Lenhard B, Wasserman WW, Sandelin A. 2010. JASPAR 2010: the greatly
907 expanded open-access database of transcription factor binding profiles. *Nucleic*
908 *acids research* **38**: D105-110.
909 Ramani V, Cusanovich DA, Hause RJ, Ma W, Qiu R, Deng X, Blau CA, Disteche CM,
910 Noble WS, Shendure J et al. 2016. Mapping 3D genome architecture through in
911 situ DNase Hi-C. *Nat Protoc* **11**: 2104-2121.
912 Rao SS, Huntley MH, Durand NC, Stamenova EK, Bochkov ID, Robinson JT, Sanborn
913 AL, Machol I, Omer AD, Lander ES et al. 2014. A 3D map of the human
914 genome at kilobase resolution reveals principles of chromatin looping. *Cell* **159**:
915 1665-1680.
916 Rebollo R, Romanish MT, Mager DL. 2012. Transposable elements: an abundant and

917 natural source of regulatory sequences for host genes. *Annu Rev Genet* **46**:
918 21-42.
919 Saeed S, Quintin J, Kerstens HH, Rao NA, Aghajanirefah A, Matarese F, Cheng SC,
920 Ratter J, Berentsen K, van der Ent MA et al. 2014. Epigenetic programming of
921 monocyte-to-macrophage differentiation and trained innate immunity. *Science*
922 *(New York, NY)* **345**: 1251086.
923 Schreiber J, Libbrecht M, Bilmes J, Noble W. 2017. Nucleotide sequence and DNaseI
924 sensitivity are predictive of 3D chromatin architecture. *bioRxiv*.
925 Shannon P, Markiel A, Ozier O, Baliga NS, Wang JT, Ramage D, Amin N, Schwikowski
926 B, Ideker T. 2003. Cytoscape: a software environment for integrated models of
927 biomolecular interaction networks. *Genome research* **13**: 2498-2504.
928 Tabuchi TM, Deplancke B, Osato N, Zhu LJ, Barrasa MI, Harrison MM, Horvitz HR,
929 Walhout AJ, Hagstrom KA. 2011. Chromosome-biased binding and gene
930 regulation by the Caenorhabditis elegans DRM complex. *PLoS Genet* **7**:
931 e1002074.
932 Wang ET, Sandberg R, Luo S, Khrebtukova I, Zhang L, Mayr C, Kingsmore SF,
933 Schroth GP, Burge CB. 2008. Alternative isoform regulation in human tissue
934 transcriptomes. *Nature* **456**: 470-476.
935 Wang J, Vicente-Garcia C, Seruggia D, Molto E, Fernandez-Minan A, Neto A, Lee E,
936 Gomez-Skarmeta JL, Montoliu L, Lunyak VV et al. 2015. MIR retrotransposon
937 sequences provide insulators to the human genome. *Proc Natl Acad Sci U S A*
938 **112**: E4428-4437.
939 Wang L, Wang S, Li W. 2012. RSeQC: quality control of RNA-seq experiments.
940 *Bioinformatics (Oxford, England)* **28**: 2184-2185.
941 Weintraub AS, Li CH, Zamudio AV, Sigova AA, Hannett NM, Day DS, Abraham BJ,
942 Cohen MA, Nabet B, Buckley DL et al. 2017. YY1 Is a Structural Regulator of
943 Enhancer-Promoter Loops. *Cell* **171**: 1573-1588 e1528.
944 Wingender E, Dietze P, Karas H, Knuppel R. 1996. TRANSFAC: a database on
945 transcription factors and their DNA binding sites. *Nucleic acids research* **24**:
946 238-241.
947 Xie Z, Hu S, Blackshaw S, Zhu H, Qian J. 2010. hPDI: a database of experimental
948 human protein-DNA interactions. *Bioinformatics (Oxford, England)* **26**:
949 287-289.

Zhang H, Li F, Jia Y, Xu B, Zhang Y, Li X, Zhang Z. 2017. Characteristic arrangement of nucleosomes is predictive of chromatin interactions at kilobase resolution. *Nucleic acids research* **45**: 12739-12751.

Zhang Y, An L, Xu J, Zhang B, Zheng WJ, Hu M, Tang J, Yue F. 2018. Enhancing Hi-C data resolution with deep convolutional neural network HiCPlus. *Nat Commun* **9**: 750.

Zhao Y, Stormo GD. 2011. Quantitative analysis demonstrates most transcription factors require only simple models of specificity. *Nature biotechnology* **29**: 480-483.